

## Article

# Friction, Wear and Corrosion Behavior of Environmentally-Friendly Fatty Acid Ionic Liquids

Javier Faes<sup>1</sup>, Rubén González<sup>1,2,\*</sup> , Antolin Hernández Battez<sup>2,3</sup> , David Blanco<sup>3</sup>, Alfonso Fernández-González<sup>4</sup> and José Luis Viesca<sup>2,3,\*</sup> 

<sup>1</sup> Department of Marine Science and Technology, University of Oviedo, 33203 Gijón, Asturias, Spain; faesjavier@uniovi.es

<sup>2</sup> Faculty of Science and Technology, Bournemouth University, Poole, Dorset BH12 5BB, UK; aehernandez@uniovi.es

<sup>3</sup> Department of Construction and Manufacturing Engineering, University of Oviedo, 33203 Gijón, Asturias, Spain; blancoadavid@uniovi.es

<sup>4</sup> Department of Physical and Analytical Chemistry, University of Oviedo, 33006 Oviedo, Asturias, Spain; fernandezgalfonso@uniovi.es

\* Correspondence: gonzalezruben@uniovi.es (R.G.); viescajose@uniovi.es (J.L.V.); Tel.: +34-985-182-350 (R.G.); +34-985-458-044 (J.L.V.)

**Abstract:** This research deals with the tribological behavior and corrosion performance of three novel fatty acid anion-based ionic liquids (FAILs): methyltrioctylammonium hexanoate ( $[N_{8,8,8,1}][C_{6,0}]$ ), methyltrioctylammonium octadecanoate ( $[N_{8,8,8,1}][C_{18,0}]$ ) and methyltrioctylammonium octadec-9-enoate ( $[N_{8,8,8,1}][C_{18,1}]$ ), employed for the first time as neat lubricant with five different material pairs: steel–steel, steel–aluminum alloy, steel–bronze, steel–cast iron and steel–tungsten carbide. These novel substances were previously obtained from fatty acids via metathesis reactions, identified structurally via NMR (nuclear magnetic resonance) and FTIR (Fourier-transform infrared spectroscopy) techniques, and then characterized from a physicochemical (density, water solubility, viscosity, viscosity index and refractive index) and environmental (bacterial toxicity and biodegradability) points of view. The corrosion behavior of the three FAILs was studied by exposure at room temperature, while friction and wear tests were performed with a reciprocating ball-on-disc configuration. The main results and conclusions obtained were: 1) Corrosion in the presence of the three FAILs is observed only on the bronze surface; 2) All FAILs presented similar tribological behavior as lubricants for each tested material pair; 3) XPS (X-ray photoelectron spectroscopy) analysis indicated that the surface behavior of the three FAILs in each material pair was similar, with low chemical interaction with the surfaces.

**Keywords:** lubrication; ionic liquids; fatty acids; wear; friction



**Citation:** Faes, J.; González, R.; Hernández Battez, A.; Blanco, D.; Fernández-González, A.; Viesca, J.L. Friction, Wear and Corrosion Behavior of Environmentally-Friendly Fatty Acid Ionic Liquids. *Coatings* **2021**, *11*, 21. <https://dx.doi.org/10.3390/coatings11010021>

Received: 30 November 2020

Accepted: 23 December 2020

Published: 27 December 2020

**Publisher's Note:** MDPI stays neutral with regard to jurisdictional claims in published maps and institutional affiliations.



**Copyright:** © 2020 by the authors. Licensee MDPI, Basel, Switzerland. This article is an open access article distributed under the terms and conditions of the Creative Commons Attribution (CC BY) license (<https://creativecommons.org/licenses/by/4.0/>).

## 1. Introduction

In 1914, Peter Walden synthesized, for the first time, the ethylammonium nitrate, an event that nowadays can be considered as the birth of ionic liquids (ILs) [1]. This important discovery was ignored for a long time, a delay that was probably related to the idea that obtaining a liquid instead of the expected solid was a sign of low purity. Ionic liquids can be defined as salts formed by the interaction between a weakly coordinating inorganic anion and an organic cation with a melting point lower than an arbitrary temperature such as 100 °C. The research interest of these salts in the liquid state began to grow in the 1970s with the synthesis of ILs from pyridinium/imidazolium cations and halide/tetrahalogenoaluminate anions, with the aim of employing them as electrolytes in batteries [2,3]. From that moment, the irruption of these novel substances led to a significant growth in research into numerous industrial applications: as solvents for both organic or inorganic materials, and in areas such as chemical synthesis, separation, extraction,

electrochemistry, nanotechnology, catalysts, liquid crystals, biotechnology, engineering, lubrication and many more up to this day [4–11].

In the last two decades, a lot of research has been carried out regarding the use of ionic liquids (ILs) in lubrication. Some properties of the ILs, such as their low flammability, inherent polarity, high thermal stability and negligible volatility, make these salts (with melting points below 100 °C) good candidates for use as a base fluid or additives [12–16]. Bhusan et al. [16] focused on the negligible volatility of ILs. This characteristic meant that contamination issues inherent to regular synthetic lubricating oils could be successfully avoided using ILs. Initially, tribological research into ionic liquids was mostly conducted using imidazolium cations and fluorine-containing anions, especially ILs composed of neutral, weakly coordinating anions such as tetrafluoroborate  $[\text{BF}_4]^-$  and hexafluorophosphate  $[\text{PF}_6]^-$  [17–25]. Jimenez et al. [22] found that imidazolium ionic liquid lubricants containing these reactive anions produce tribochemical interactions at the aluminum–steel interface. Therefore, these fluorine-based anions tend to produce corrosion in the presence of water, as the hydrolysis products of these substances are highly corrosive and toxic [26–29]. Freire et al. [29] explained that this issue is mainly produced under certain experimental conditions of pH and temperature. This known issue led to research into novel and more stable fluorine-containing anions, such as  $[\text{FAP}]^-$  and  $[\text{NTf}_2]^-$  [30–49]. Minami et al. [49] worked with several ionic liquids with the  $[\text{NTf}_2]^-$  anion, finding a mixture of phosphate and fluoride protective boundary films due to tribochemical reactions occurring at the surface.

Due to the high cost of ILs, most of the studies related to their use in lubrication have focused on their utilization as additives, especially ammonium and phosphonium cation-based ILs, due to their good solubility in common base oils [23,36,50–60]. However, the use of ILs as a neat lubricant could be proposed for tribological pairs under severe conditions such as high temperature, high load, high vacuum, corrosive environment and low-pressure applications in which traditional lubricants do not perform properly [14,15,27,48,57]. Otero et al. [54] studied the tribological performance of two phosphonium cation-based ionic liquids:  $[\text{P}_{6,6,6,14}][(\text{C}_2\text{F}_5)_3\text{PF}_3]$  and  $[\text{P}_{4,4,4,2}][\text{C}_2\text{C}_2\text{PO}_4]$  as neat or lubricants' additives in steel–steel contact, with XPS analysis revealing the formation of tribofilms on the worn surface of both ILs, mainly composed of iron phosphides and oxides. García et al. [27] compared the tribological behavior of  $[\text{HEIM}][\text{PF}_6]$  ionic liquid versus a polyalphaolefin (PAO) base oil in steel–steel contact, finding that the protective layer of the absorbed IL film on the steel surface is responsible for the improved tribological behavior of the IL with respect to the PAO. Therefore, steel–steel contact has been the material pair most frequently used in the abovementioned studies, probably due to the widespread use of steel in industry [17,19,35,61–65]. Liu et al. [17] showed that ILs formed a  $\text{FeF}_2$  and  $\text{B}_2\text{O}_3$  surface protective film which contributes to low friction and wear under steel–steel lubricated contact. However, other materials used in engineering applications, such as aluminum, silicon, titanium, copper, sialon ceramics, and different coatings, have also been tested when lubricated with ILs [38,39,66–77]. Qu et al. [66] reported the tribological performance of two  $[\text{NTf}_2]^-$  ILs in comparison with formulated SAE 15W40 engine oil, obtaining up to 20% lower COF for different aluminum alloys with a uniform counterpart of AISI 52100 steel.

In addition to facing problems related to the price and solubility of ILs, research is currently directed towards obtaining more environmentally-friendly ILs (without halogens or metals in their composition) [78,79]. The possibility of creating tailored ILs through the combination of existing ions via synthesis is leading to new IL families with improvements in terms of toxicity and biodegradability [80–83]. Among these new ILs are fatty acid anion-based ionic liquids (FAILs), reported for the first time in 2013 [84], and whose use in lubrication studies has greatly increased [85–105]. Gusain et al. [87] proved that several FAILs used as lubricants provide between 20 and 50% COF reduction compared to that of polyol ester base oil, forming a stable tribochemical thin film with the steel surface under boundary lubrication, probably related to the inherent polar nature of these substances.

Finally, a research study [95] using three novel FAILs synthesized for lubrication purposes found that the alkyl chain length of the anion affects the chemical composition of the worn surface during tribological tests in four different material pairs (steel–steel, steel–aluminum alloy, steel–bronze and steel–tungsten carbide). Following this research line regarding the alkyl chain length effect, this study deals with three new fatty acid anion-based ionic liquids (FAILs): methyltrioctylammonium hexanoate ( $[N_{8,8,8,1}][C_{6:0}]$ ), methyltrioctylammonium octadecanoate ( $[N_{8,8,8,1}][C_{18:0}]$ ) and methyltrioctylammonium octadec-9-enoate ( $[N_{8,8,8,1}][C_{18:1}]$ ), synthesized from natural sources and employed for the first time as neat lubricant in five material pairs (four of them used before [95]).

## 2. Materials and Methods

### 2.1. Ionic Liquids and Materials

A previously described salt metathesis reaction method was employed to synthesize the three novel ionic liquids derived from fatty acids [104]. Sodium hydroxide, ethanol solution (70% w/w) and toluene (99.8%) were used as chemical reagents for the synthesis, as well as methyltrioctylammonium bromide ionic liquid ( $[N_{8,8,8,1}][Br]$ ) (>97%) as cation precursor, and hexanoic, stearic and oleic acids (natural >98%) as anion precursors. All these reagents were provided by Sigma-Aldrich S.A., and used without further purification. The chemical description of the methyltrioctylammonium hexanoate ( $[N_{8,8,8,1}][C_{6:0}]$ ), methyltrioctylammonium octadecanoate ( $[N_{8,8,8,1}][C_{18:0}]$ ) and methyltrioctylammonium octadec-9-enoate ( $[N_{8,8,8,1}][C_{18:1}]$ ) ionic liquids is shown in Table 1. The pH measurements were conducted using pH indicator strips.

**Table 1.** Chemical description of the FAILs (fatty acid anion-based ionic liquids) used in this work.

IUPAC Name	Acronym	Empirical Formula	pH	Chemical Structures
Methyltrioctylammonium hexanoate	$[N_{8,8,8,1}][C_{6:0}]$	$C_{31}H_{65}NO_2$	8–9	
Methyltrioctylammonium octadecanoate	$[N_{8,8,8,1}][C_{18:0}]$	$C_{43}H_{89}NO_2$	8–9	
Methyltrioctylammonium octadec-9-enoate	$[N_{8,8,8,1}][C_{18:1}]$	$C_{43}H_{87}NO_2$	8–9	

In previous work, Fourier-transform infrared spectroscopy (FTIR) and  $^1H$  and  $^{13}C$  nuclear magnetic resonance (NMR) analysis were employed in order to identify the molecular structures of the three FAILs [92]. The bacterial toxicity and biodegradability of the ILs and the relationship with their density, water solubility, viscosity, viscosity index and refractive index were also previously studied [97].

Five different materials have been chosen in order to evaluate the lubricant properties of the FAILs. Discs (10 mm in diameter, 3 mm-thick) of tungsten carbide WC6Co (hardness 1843 HV<sub>0.3</sub> and surface roughness Ra < 0.022 μm), cast iron BS1452 grade 240 (hardness 225 HV<sub>0.1</sub> and surface roughness Ra < 0.053 μm), bronze PB1 BS 1400 (hardness 219 HV<sub>0.1</sub> and surface roughness Ra < 0.027 μm), aluminum 6082 T6 (hardness 116 HV<sub>0.1</sub> and surface roughness Ra < 0.025 μm) and AISI 52100 steel (hardness 225 HV<sub>0.1</sub> and surface roughness Ra < 0.018 μm) have been used to test corrosion, friction and wear behavior of the three FAILs. The chemical composition of these materials can be found in Table 2. The wetting properties of these FAILs on the abovementioned materials have been also previously reported [92].

**Table 2.** Chemical composition (%) of the five materials studied.

Material	Chemical Composition (%)
Tungsten Carbide WC6Co	WC: 94; Co: 6.
Cast iron BS1452	C: 2.90–3.65; Si: 1.80–2.90; Mn:0.40–0.70; S: 0.10; P: 0.30; Fe: balance
Bronze PB1 BS 1400	Sn: 10–12; Zn: 0.05; Ni: 0.10; Pb: 0.25; P: 0.5–1.2; Al 0.005; Fe: 0.10; Cu: balance
Aluminum 6082 T6	Mn: 0.40–1.00; Fe: 0.0–0.50; Mg: 0.60–1.20; Si: 0.70–1.30; Cu: 0.0–0.10; Zn: 0.0–0.20; Ti: 0.0–0.10; Cr: 0.0–0.25; Al: balance
AISI 52100 Steel	C: 0.93–1.05; Mn: 0.25–0.45; P: 0.015; Si: 0.15–0.35; Ni: 0.25; Cr: 1.35–1.60; Cu: 0.30; Mo: 0.10

## 2.2. Corrosion Study

The corrosion activity of the FAILs on the five materials was evaluated by depositing 5  $\mu$ L of the corresponding FAIL on the surface of the discs (Figure 1), which were exposed in air at room temperature with a relative humidity of 50–65% for three weeks. The discs were previously cleaned with heptane in an ultrasound bath and dried with hot air. At the end of the corrosion test, the disc surfaces were cleaned again with heptane in the ultrasound bath for 10 min and then analyzed by two complementary methods. Initially, a simple visual inspection of the surface of the discs was made, and then scanning electron microscopy and energy dispersive spectroscopy (SEM-EDS) was employed to determine the presence of corrosion.

**Figure 1.** Schematic diagram of the corrosion tests.

## 2.3. Tribological Tests

Five different tribological pairs were tested in a reciprocating ball-on-disc configuration (Figure 2). AISI 52100 steel balls (6 mm in diameter,  $R_a < 0.05$  mm, HRC 58–66) were run against discs of tungsten carbide (WC6Co), cast iron (BS1452 240), bronze (PB1 BS 1400), aluminum (6082 T6) and steel (AISI 52100), respectively. All tests were carried out in a Bruker UMT3 tribometer (Billerica, MA, USA) with a duration of 30 min, at 25 °C and a relative humidity between 50 and 65%, at a frequency of 15 Hz, stroke length of 4 mm and load of 50 N (corresponding to a mean contact pressure of 1.03 GPa for the steel–aluminum pair, 1.62 GPa for the steel–steel pair, 2.14 GPa for the steel–WC pair, 1.29 GPa for the steel–cast iron pair, and 1.22 GPa for the steel–bronze pair). At the beginning of each test, 25  $\mu$ L of the corresponding FAIL were deposited in the ball-disc contact. At the end of tests, the specimens were cleaned with heptane in an ultrasound bath for 5 min, rinsed in ethanol and dried with hot air. At least two replicates of each test were made. The friction coefficient was measured during tests.

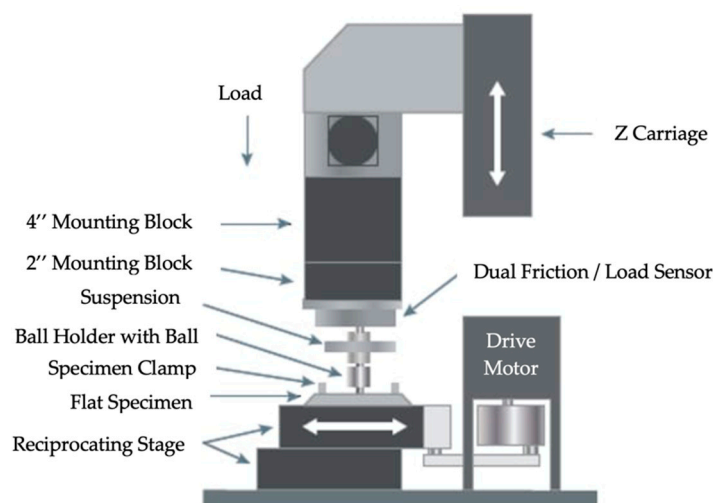


**Figure 2.** Configuration of the tribological tests.

#### 2.4. Surface Analysis

After corrosion and tribological tests, the disc surfaces were analyzed by scanning electron microscopy and energy dispersive spectroscopy (SEM-EDS). A JEOL JSM 5600 microscope (Akishima, Tokyo, Japan) equipped with an X-ray Energy-dispersive Microanalyser, Oxford, mod Inca Energy 200 was employed. Its characteristics include: acceleration voltage from 0.5 to 30 kV, magnification from 18 to 300.000 with WD of 48 mm,  $2.560 \times 1.920$  image scanning, detection area of  $10 \text{ mm}^2$ , resolution of 138 eV, with an elemental detection range that goes from Be to U. Its software allows for element mapping, analysis of the elemental distribution, spectra comparison and a relatively precise quantification. These analyses were semi-quantitative and were made in order to detect surface alterations and determine the predominant wear mechanism. Additionally, wear scars on the disc surfaces were studied by X-ray photoelectron spectroscopy (XPS) to evaluate the surface-IL interaction. A photoelectron spectrometer (SPECS) with a hemispherical energy analyzer (Phoibos type) was employed.

### 3. Results and Discussion

#### 3.1. Corrosion Study

Figure 3 shows images of the evolution of the surfaces of the different materials during corrosion testing. As can be seen, no sign of corrosion activity could be observed on most of the studied surfaces after 21 days of testing. Only the bronze surface changed as a result of its interaction with the  $[\text{N}_{8,8,8,1}][\text{C}_{18:0}]$  and  $[\text{N}_{8,8,8,1}][\text{C}_{18:1}]$  ILs. These results were later confirmed by SEM-EDS, since changes were not found on the surface or in the EDS spectra of steel, aluminum, cast iron and WC. On the other hand, surface modifications were observed for bronze (Figure 4) after 21 days exposed to  $[\text{N}_{8,8,8,1}][\text{C}_{18:0}]$  and  $[\text{N}_{8,8,8,1}][\text{C}_{18:1}]$ . The EDS revealed a high oxygen content (Table 3) on bronze surface exposed to the two abovementioned FAILs, which is indicative of oxidation phenomena.

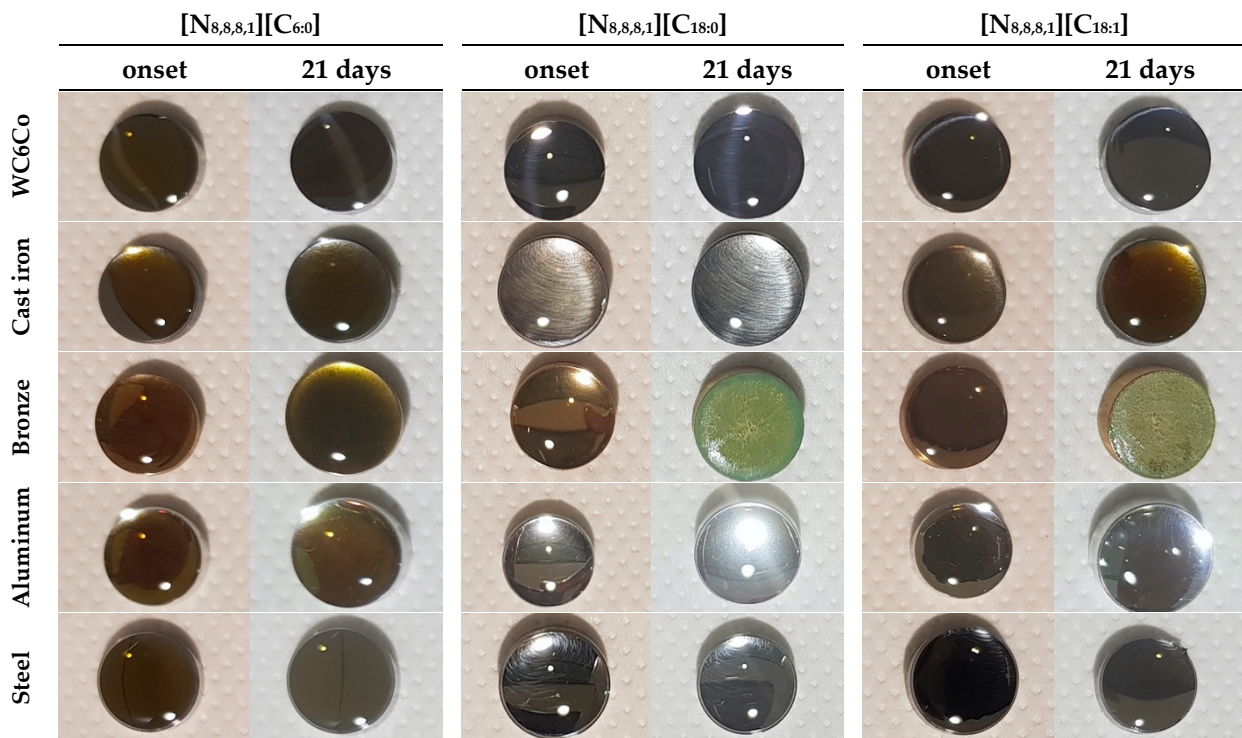


Figure 3. Disc surfaces at the beginning and end of corrosion tests.

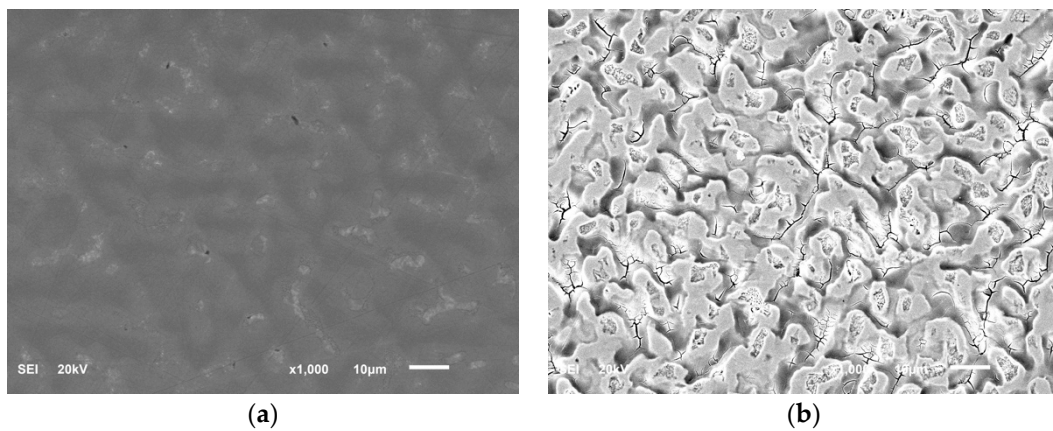


Figure 4. Bronze surface: (a) clean. (b) after 21 days in the presence of  $[N_{8,8,8,1}][C_{18:1}]$ .

Table 3. EDS (energy dispersive spectroscopy) analysis of bronze surface (at concentration, %) before and after corrosion tests with  $[N_{8,8,8,1}][C_{18:0}]$  and  $[N_{8,8,8,1}][C_{18:1}]$  FAIL.

Corrosion Tests		C	O	Cu	Sn	Total
Before	Clean	19.84	-	75.45	4.71	100.00
After (21 days)	$[N_{8,8,8,1}][C_{18:0}]$	22.56	19.76	47.63	10.05	100.00
	$[N_{8,8,8,1}][C_{18:1}]$	19.58	26.44	38.38	15.60	100.00

### 3.2. Tribological Test

Figure 5 shows the evolution of the coefficient of friction during tribological tests carried out for each of the five material pairs. Additionally, the average values of the coefficient of friction obtained for every surface–FAIL combination are also included. In general, the friction coefficient remains steady during the tests, with an appreciable decrease only being detected during testing with the steel–aluminum pair lubricated with

$[N_{8,8,8,1}][C_{6:0}]$ , probably due to the running-in process. The different friction coefficients obtained for the five material pairs can be related to the hardness of the lower specimen (disc). Likewise, the roughness and the Young's modulus values of the five materials also led to friction differences. The higher the Young's modulus, the higher the Hertz contact pressures, which results in lower lubricant film thicknesses, with the corresponding friction increase. The tungsten carbide–steel pair showed the highest friction value of the five material pairs tested, aluminum–steel showed the lowest, while steel–steel had an intermediate result. All these results are in agreement with their Hertz contact pressures.

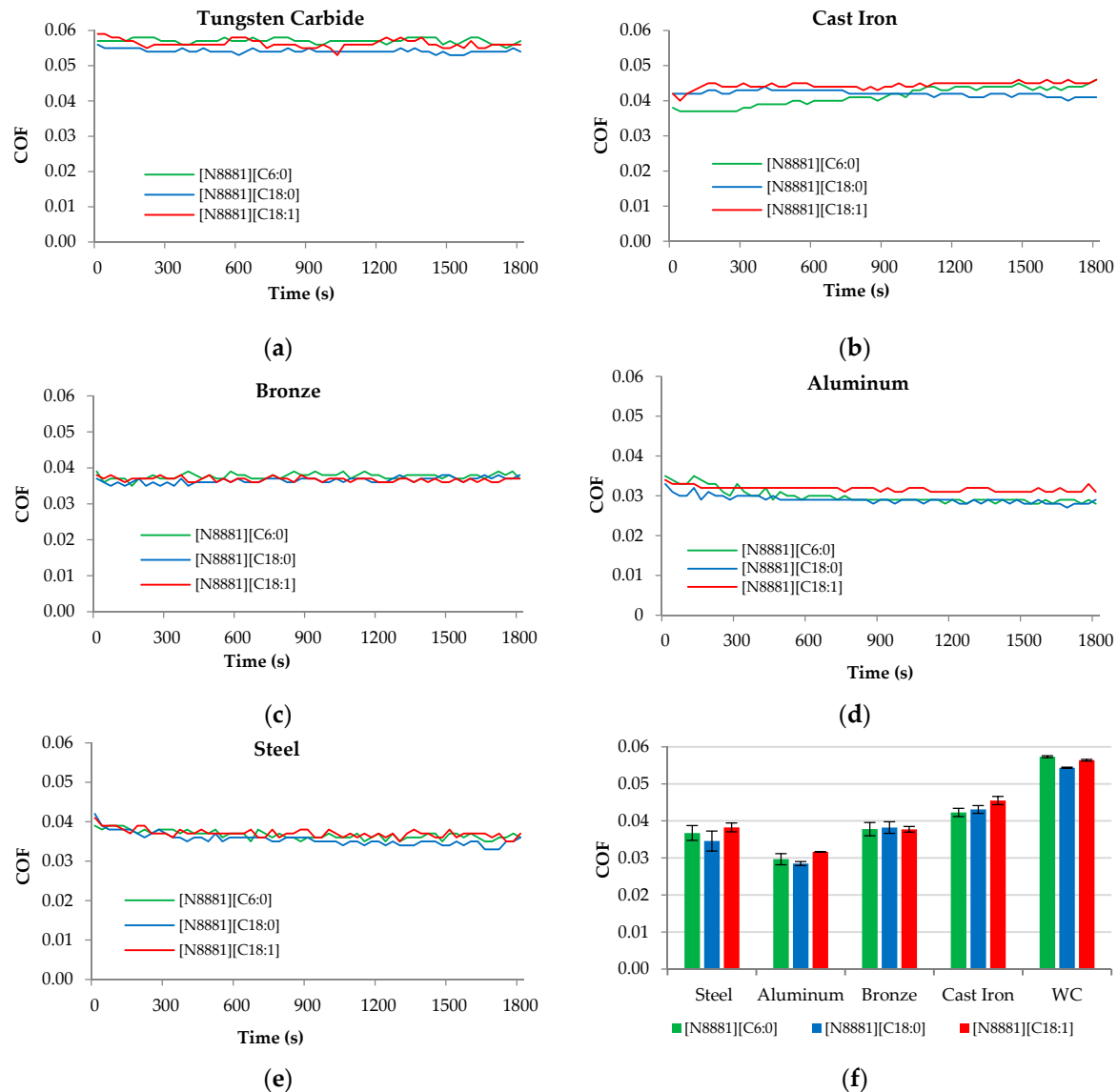


**Figure 5.** Coefficient of friction(COF) versus testing time and average COF for all tests. (a) Tungsten carbide surface. (b) Cast iron surface. (c) Bronze surface. (d) Aluminum surface. (e) Steel surface. (f) Average coefficients of friction on all surfaces.

Regarding FAILs, all of them exhibited similar friction behavior when used as lubricant for the same material pairs, although the  $[N_{8,8,8,1}][C_{18:0}]$  exhibited slightly lower friction values on steel, aluminum and tungsten carbide. In general, friction values obtained when testing with  $[N_{8,8,8,1}][C_{18:1}]$  were higher than those obtained with  $[N_{8,8,8,1}][C_{18:0}]$ .

Table 4 shows the average wear for all the tests that were carried out. The measured values for tungsten carbide indicate almost negligible wear compared to the other surfaces; the  $[N_{8,8,8,1}][C_{18:0}]$  FAIL showing the lowest wear for this material. Of the other four

materials, the steel–steel pair exhibited lower wear values than those of aluminum, bronze and cast iron, which had similar characteristics in this respect. No significant differences between the use of one FAIL or another as a lubricant could be indicated, although in the case of aluminum, bronze and WC, measured wear was higher on surfaces lubricated with  $[\text{N}_{8,8,8,1}][\text{C}_{6:0}]$  than those lubricated with  $[\text{N}_{8,8,8,1}][\text{C}_{18:0}]$  and  $[\text{N}_{8,8,8,1}][\text{C}_{18:1}]$ .

**Table 4.** Wear volume ( $\times 10^6 \mu\text{m}^3$ ).

FAIL	$[\text{N}_{8,8,8,1}][\text{C}_{6:0}]$		$[\text{N}_{8,8,8,1}][\text{C}_{18:0}]$		$[\text{N}_{8,8,8,1}][\text{C}_{18:1}]$	
	Average Value	Standard Deviation	Average Value	Standard Deviation	Average Value	Standard Deviation
WC	0.275168	0.009613	0.078149	0.009957	0.214120	0.010297
Cast Iron	9.205816	0.018750	8.198145	1.045135	7.871593	1.150991
Bronze	8.957983	0.774445	9.277544	0.967261	7.536865	0.834904
Aluminum	8.235090	0.557433	6.949583	0.002316	7.763727	0.037912
Steel	6.472298	0.146255	6.558970	0.075222	7.036670	0.086427

### 3.3. Surface Analysis

Figure 6 shows SEM images of the worn surfaces before and after tribological tests. As can be seen, no marked differences were found between ILs in the lubrication of each material pair. According to the above wear volume results, no appreciable surface damage could be detected on WC surfaces after tribological tests. These results and the previously described friction values obtained for this surface indicate that the antiwear behavior of tungsten carbide is more related to its hardness than to the viscosity and surface–IL tribochemical interactions. For the rest of the materials, a well-defined wear scar could be observed on the surface; this plastic deformation indicating adhesion as the predominant wear mechanism. Aluminum, bronze and steel showed a smooth worn surface, while cast iron also exhibited signs of abrasion. However, a slightly greater wear scar was detected after tests when bronze was lubricated with  $[\text{N}_{8,8,8,1}][\text{C}_{18:0}]$ . In the case of aluminum, the wear scar and wear volume were not as big as might be expected from its low hardness. This may be due to a rapid initial increase in the contact area with the consequent reduction of the Hertz contact pressure, which favors a thicker lubricant film. Such a sequence of events would also explain the low friction values observed in steel–aluminum. Regarding the EDS analysis, only the elements present in the different materials were detected on the worn surfaces.

Figure 7 shows the high resolution N1s spectra from the XPS analysis for samples tested with  $[\text{N}_{8,8,8,1}][\text{C}_{6:0}]$ . The N1s content of bronze and aluminum surfaces is too low to allow an analysis of the peaks, and the N1s peak for the other three samples appears between 399.4 eV and 399.6 eV, which is definitively much lower than the binding energy described for the  $[\text{N}_{8,8,8,1}]^+$  cation in different ionic liquids, which lies at around 402 eV [106]. However, the position also seems a little high to be a metal nitride, since these have been described as having peaks at around 398 eV (FeN [107]) and 397.8 eV ( $\text{W}_3\text{N}_4$  [108]). The position of the peak could be due to a partially degraded cation adsorbed onto the surface.



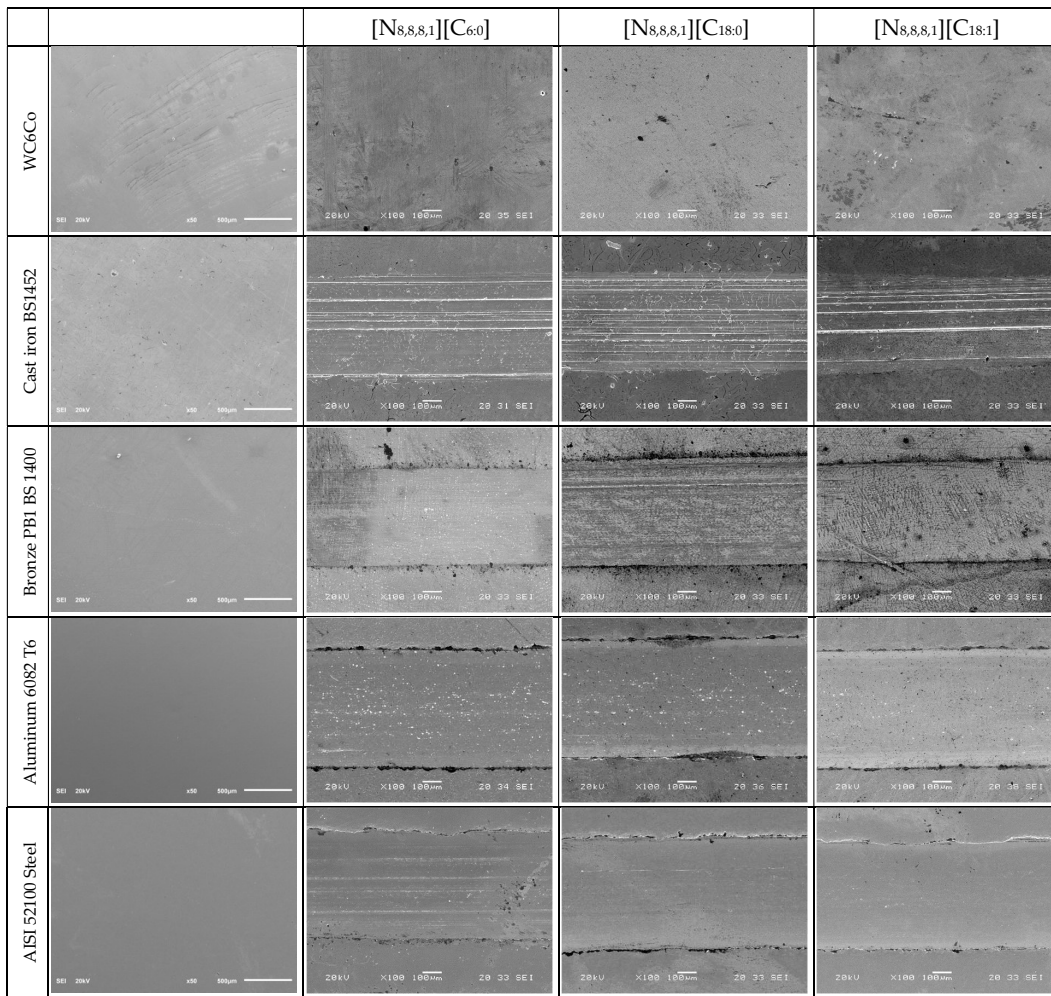


Figure 6. Micrographs of wear scars on the different discs after tribological tests with FAIL lubrication.

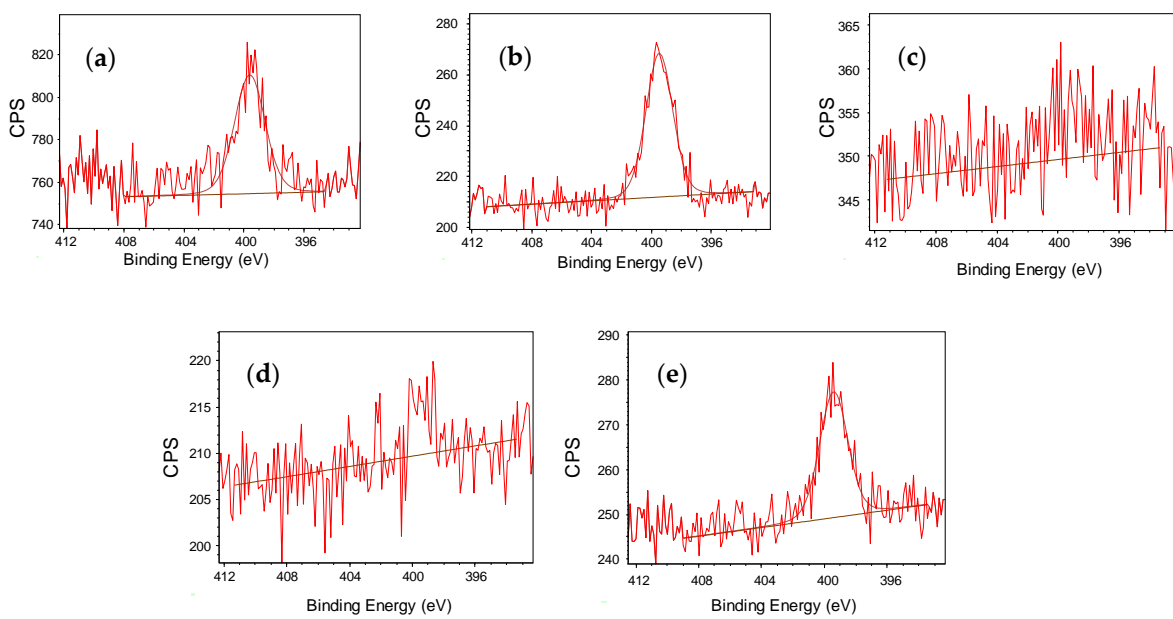
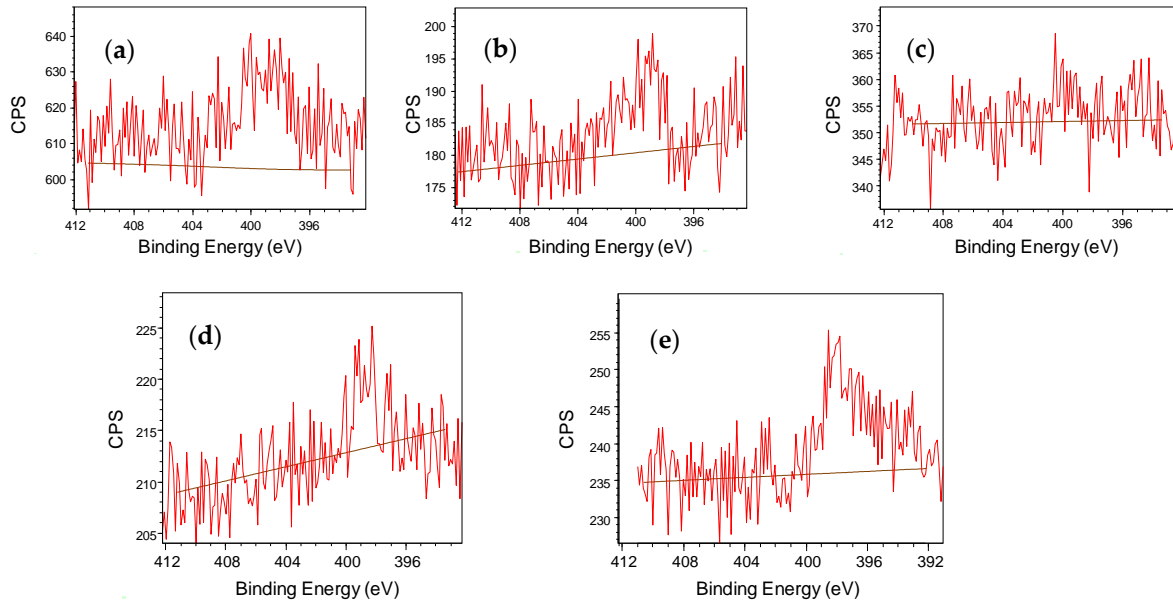
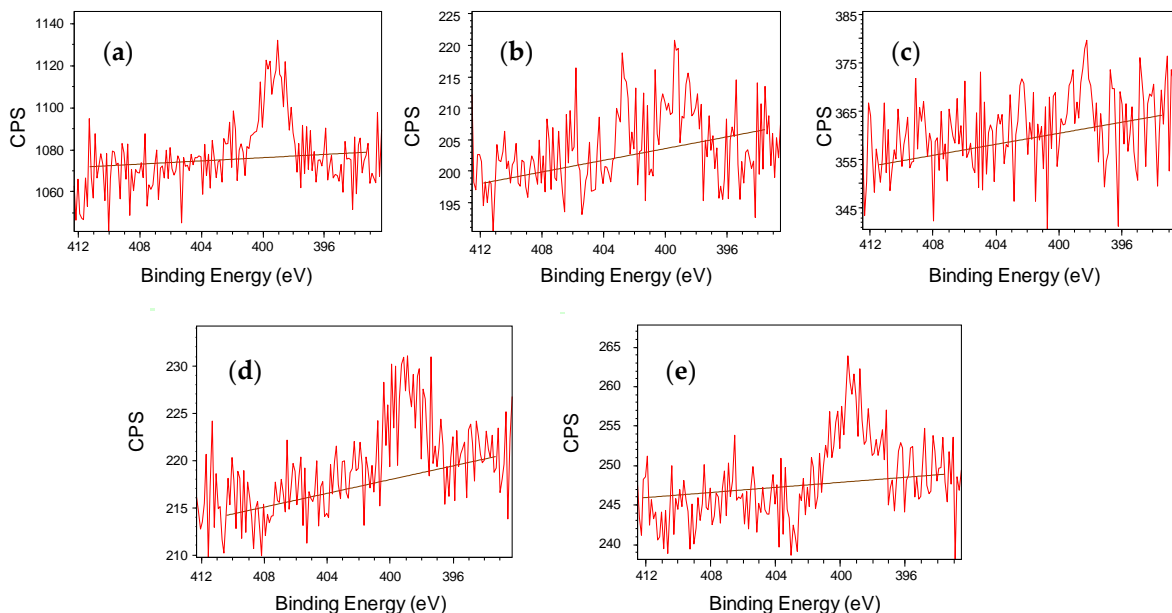


Figure 7. N<sub>1s</sub> spectra for the different samples lubricated with [N<sub>8,8,8,1</sub>][C<sub>6:0</sub>]. Images correspond to: (a) WC, (b) cast iron, (c) bronze, (d) aluminum and (e) steel.

It is interesting that the signal-to-noise ratio in the case of samples tested with  $[N_{8,8,8,1}][C_{18:0}]$  and  $[N_{8,8,8,1}][C_{18:1}]$  is very poor in every case (Figures 8 and 9), suggesting that the interaction between the ionic liquid and the surface is weaker.



**Figure 8.** N1s spectra for the different samples lubricated with  $[N_{8,8,8,1}][C_{18:0}]$ . Images correspond to: (a) WC, (b) cast iron, (c) bronze, (d) aluminum and (e) steel.



**Figure 9.** N1s spectra for the different samples lubricated with  $[N_{8,8,8,1}][C_{18:1}]$ . Images correspond to: (a) WC, (b) cast iron, (c) bronze, (d) aluminum and (e) steel.

The surface was also studied by investigating the main element in each case (Fe for cast iron and steel, Al for aluminum, W for tungsten carbide and Cu and Sn for bronze), and the high resolution spectra of these elements after testing with each different lubricant were compared. In the case of steel (Figure 10a),  $[N_{8,8,8,1}][C_{18:0}]$  shows a difference when compared to  $[N_{8,8,8,1}][C_{6:0}]$  or  $[N_{8,8,8,1}][C_{18:1}]$ , consisting in a peak shift towards lower binding energies, which usually indicates a lower degree of oxidation. However, taking

into account the insignificant differences in the friction coefficient or wear volume of the steel samples tested, the difference that was found does not seem to be significant. This difference does not appear in cast iron (Figure 10b), where the three surfaces seem to be very similar.

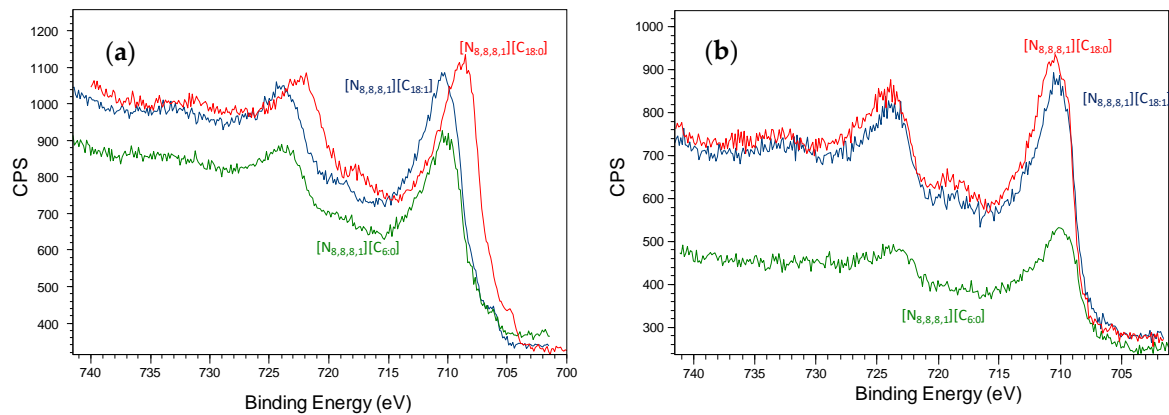


**Figure 10.** Fe2p high resolution spectra in: (a) steel and (b) cast iron compared for the three ionic liquids.

Regarding the chemical composition of the other tested surfaces (Figure 11), the ionic liquid seems only to cause a difference to the surface in the case of tungsten carbide, although this is not reflected in significant changes in the tribological properties.

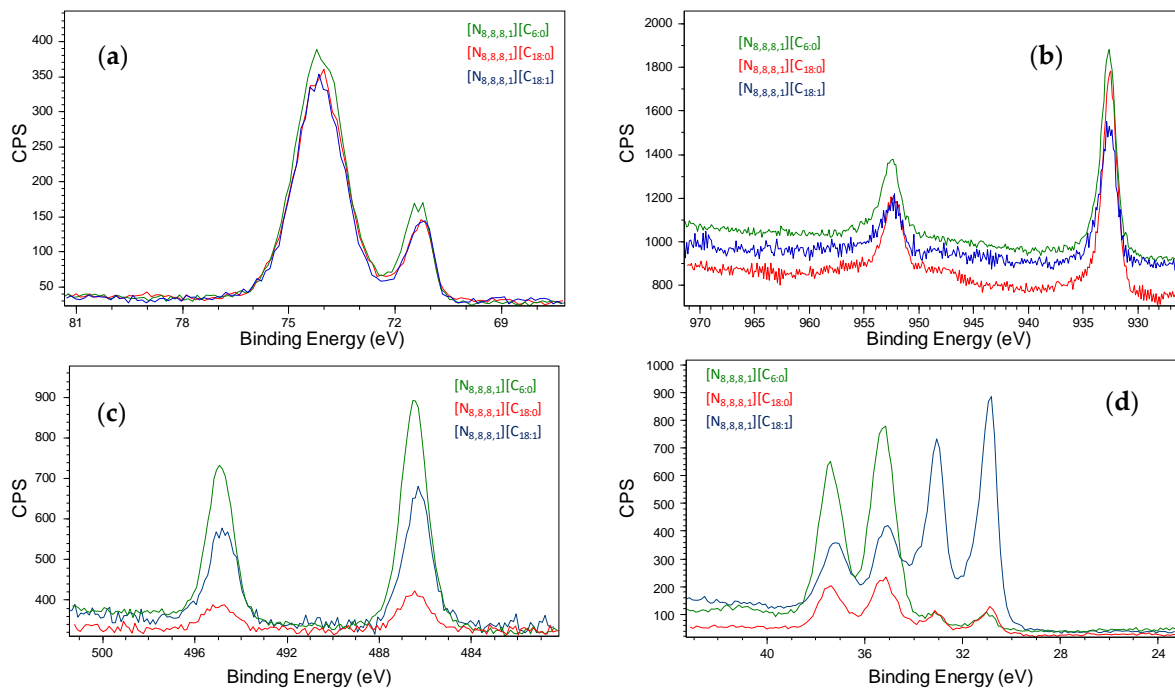


**Figure 11.** (a) Al2p, (b) Cu2p, (c) Sn3d and (d) W4f high resolution spectra for aluminum, bronze and WC surfaces.

The position of the tungsten 4f7/2 doublets is between 31.0 and 31.1 eV for the first doublet and between 34.9 and 35.3 eV for the second. The one at the lowest binding energies is interpreted as tungsten carbide by some authors, who described it around 30.2–32.4 eV [109], but also as W by other authors [110]. The highest binding energies correspond to a more oxidized tungsten carbide, which is probably WO<sub>3</sub> [99]. According to this explanation, it seems that the longer the carbon chain of the anion, the lower is the oxidation suffered by the surface. Thus, [N<sub>8,8,8,1</sub>][C<sub>18,1</sub>] shows the highest WC/WO<sub>3</sub> ratio

whereas  $[N_{8,8,8,1}][C_{6:0}]$  shows the lowest one. However, this antioxidant capability does not seem to affect the tribological properties, as no CoF or wear differences can be seen between WC samples.

#### 4. Conclusions

The use of three methyltrioctylammonium cation-based fatty acid ionic liquids (FAILs) as pure lubricants in five tribological pairs (steel–steel, steel–cast iron, steel–aluminum, steel–bronze and steel–tungsten carbide) have been studied. After the research, the following conclusions can be drawn:

- A corrosion phenomenon could be observed in the bronze surface in the presence of the three FAILs. However, for the rest of the materials, no surface modification appeared after corrosion tests.
- The three FAILs presented similar tribological behavior, without notable differences in friction and wear values registered, when used as lubricant with each tested material pair.
- The low wear recorded for the tungsten carbide–steel pair is more related to its hardness than to its interaction with FAILs. The higher friction values found in this case are linked to its higher contact pressure.
- For the aluminum–steel pair, a low coefficient of friction was recorded as a result of the low contact pressure that favored better lubrication.
- The XPS analysis indicated that the behavior of the three FAILs in each material pair was similar, with low chemical interaction with the surfaces.

**Author Contributions:** Conceptualization, A.H.B., J.L.V. and R.G.; methodology, J.L.V. and J.F.; validation, D.B., J.F. and A.F.-G.; investigation, J.F., A.F.-G. and D.B.; resources, A.H.B. and J.L.V.; writing—original draft preparation, J.F., R.G. and A.F.-G.; writing—review and editing, J.L.V., A.H.B. and R.G.; visualization, D.B., J.F. and A.F.-G.; supervision, J.L.V.; project administration, A.H.B. and R.G.; funding acquisition, J.L.V., A.H.B. and R.G. All authors have read and agreed to the published version of the manuscript.

**Funding:** This research was funded by the Spanish Ministry of Economy and Competitiveness (MINECO-17-DPI2016-79690-R) and by the Foundation for the Promotion in Asturias of Applied Scientific Research and Technology (FC-GRUPIN-IDI/2018/000131).

**Acknowledgments:** The authors would like to thank the Electron Microscopy Unit of the Scientific-Technical Services at the University of Oviedo.

**Conflicts of Interest:** The authors declare no conflict of interest.

#### References

1. Walden, P. Molecular weights and electrical conductivity of several fused salts. *Bull. Imp.Acad. Sci. (St. Petersburg)* **1914**, *8*, 405–422.
2. Chum, H.L.; Koch, V.; Miller, L.; Osteryoung, R. Electrochemical scrutiny of organometallic iron complexes and hexamethylbenzene in a room temperature molten salt. *J. Am. Chem. Soc.* **1975**, *97*, 3264–3265. [[CrossRef](#)]
3. Wilkes, J.S.; Levisky, J.A.; Wilson, R.A.; Hussey, C.L. Dialkylimidazolium chloroaluminate melts: A new class of room-temperature ionic liquids for electrochemistry, spectroscopy and synthesis. *Inorg. Chem.* **1982**, *21*, 1263–1264. [[CrossRef](#)]
4. Wilkes, J.S.; Zaworotko, M.J. Air and water stable 1-ethyl-3-methylimidazolium based ionic liquids. *Chem. Commun.* **1992**, *13*, 965–967. [[CrossRef](#)]
5. Wassercheid, P.; Welton, T. *Ionic Liquid in Synthesis*, 2nd ed; Wiley: Weinheim, Germany, 2008.
6. Olivier, H. Recent developments in the use of non-aqueous ionic liquids for two-phase catalysis. *J. Mol. Catal. A Chem.* **1999**, *146*, 285–289. [[CrossRef](#)]
7. Hagiwara, R.; Ito, Y. Room temperature ionic liquids of alkyimidazolium cations and fluoroanions. *J. Fluor. Chem.* **2000**, *105*, 221–227. [[CrossRef](#)]
8. Welton, T. Room-temperature ionic liquids, solvents for synthesis and catalysis. *Chem. Rev.* **1999**, *99*, 2071–2084. [[CrossRef](#)]
9. Keskin, S.; Kayrak-Talay, D.; Akman, U.; Hortaçsu, Ö. A review of ionic liquids towards supercritical fluid applications. *J. Supercrit. Fluids* **2007**, *43*, 150–180. [[CrossRef](#)]
10. Berthod, A.; Angel, M.J.R.; Carda-Broch, S. Ionic liquids in separation techniques. *J. Chromatogr. A* **2008**, *1184*, 6–18. [[CrossRef](#)]

11. Zhou, F.; Liang, Y.; Liu, W. Ionic liquid lubricants: Designed chemistry for engineering applications. *Chem. Soc. Rev.* **2009**, *38*, 2590–2599. [[CrossRef](#)]
12. Ye, C.F.; Liu, W.M.; Chen, Y.X.; Yu, L.G. Room-temperature ionic liquids: A novel versatile lubricant. *Chem Commun (Cambridge)* **2001**, *21*, 2244–2245. [[CrossRef](#)] [[PubMed](#)]
13. Minami, I. Ionic liquids in tribology. *Molecules* **2009**, *14*, 2286–2305. [[CrossRef](#)] [[PubMed](#)]
14. Bermúdez, M.D.; Jiménez, A.E.; Sanes, J.; Carrión, F.J. Ionic liquids as advanced lubricant fluids. *Molecules* **2009**, *14*, 2888–2908. [[CrossRef](#)] [[PubMed](#)]
15. Somers, A.; Howlett, P.; MacFarlane, D.; Forsyth, M. A review of ionic liquid lubricants. *Lubricants* **2013**, *1*, 3–21. [[CrossRef](#)]
16. Palacio, M.; Bhushan, B. A review of ionic liquids for green molecular lubrication in nanotechnology. *Tribol. Lett.* **2010**, *40*, 247–268. [[CrossRef](#)]
17. Liu, W.; Ye, C.; Gong, Q.; Wang, H.; Wang, P. Tribological performance of room-temperature ionic liquids as lubricant. *Tribol. Lett.* **2002**, *13*, 81–85. [[CrossRef](#)]
18. Chen, Y.M.; Zeng, Z.X.; Yang, S.R.; Zhang, J.Y. The tribological performance of BCN films under ionic liquids lubrication. *Diam. Relat. Mater.* **2009**, *18*, 20–26. [[CrossRef](#)]
19. Sanes, J.; Carrión, F.J.; Bermúdez, M.D.; Martínez-Nicolás, G. Ionic liquids as lubricants of polystyrene and polyamide 6-steel contacts. Preparation and properties of new polymer-ionic liquid dispersions. *Tribol. Lett.* **2006**, *21*, 121. [[CrossRef](#)]
20. Kamimura, H.; Kubo, T.; Minami, I.; Mori, S. Effect and mechanism of additives for ionic liquids as new lubricants. *Tribol. Int.* **2007**, *40*, 620–625. [[CrossRef](#)]
21. Qu, J.; Truhan, J.J.; Dai, S.; Luo, H.; Blau, P.J. Ionic liquids with ammonium cations as lubricants or additives. *Tribol. Lett.* **2006**, *22*, 207–214. [[CrossRef](#)]
22. Jiménez, A.E.; Bermúdez, M.D.; Iglesias, P.; Carrión, F.J.; Martínez-Nicolás, G. 1-N-alkyl -3-methylimidazolium ionic liquids as neat lubricants and lubricant additives in steel–aluminium contacts. *Wear* **2006**, *260*, 766–782. [[CrossRef](#)]
23. Hernández Battez, A.; González, R.; Viesca, J.L.; Blanco, D.; Asedegbega, E.; Osorio, A. Tribological behaviour of two imidazolium ionic liquids as lubricant additives for steel/steel contacts. *Wear* **2009**, *266*, 1224–1228. [[CrossRef](#)]
24. Phillips, B.S.; John, G.; Zabinski, J.S. Surface chemistry of fluorine containing ionic liquids on steel substrates at elevated temperature using Mössbauer spectroscopy. *Tribol. Lett.* **2007**, *26*, 85–91. [[CrossRef](#)]
25. Mu, Z.; Liu, W.; Zhang, S.; Zhou, F. Functional room-temperature ionic liquids as lubricants for an aluminum-on-steel system. *Chem. Lett.* **2004**, *33*, 524–525. [[CrossRef](#)]
26. Torimoto, T.; Tsuda, T.; Okazaki, K.I.; Kuwabata, S. New frontiers in materials science opened by ionic liquids. *Adv. Mater.* **2010**, *22*, 1196–1221. [[CrossRef](#)]
27. García, A.; González, R.; Hernández Battez, A.; Viesca, J.L.; Monge, R.; Fernández-González, A.; Hadfield, M. Ionic liquids as a neat lubricant applied to steel-steel contacts. *Tribol. Int.* **2014**, *72*, 42–50. [[CrossRef](#)]
28. Uerdingen, M.; Treber, C.; Balsler, M.; Schmitt, G.; Werner, C. Corrosion behaviour of ionic liquids. *Green Chem.* **2005**, *7*, 321. [[CrossRef](#)]
29. Freire, M.G.; Neves, C.M.S.S.; Marrucho, I.M.; Coutinho, J.A.P.; Fernandes, A.M. Hydrolysis of tetrafluoroborate and hexafluorophosphate counter ions in imidazolium-based ionic liquids. *J. Phys. Chem. A* **2009**, *114*, 3744–3749. [[CrossRef](#)]
30. González, R.; Hernández Battez, A.; Blanco, D.; Viesca, J.L.; Fernández-González, A. Lubrication of TiN, CrN and DLC PVD coatings with 1-butyl-1-methylpyrrolidinium tris(pentafluoroethyl)trifluorophosphate. *Tribol. Lett.* **2010**, *40*, 269–277. [[CrossRef](#)]
31. Blanco, D.; González, R.; Hernández Battez, A.; Viesca, J.L.; Fernández-González, A. Use of ethyl-dimethyl-2-methoxyethylammonium tris(pentafluoroethyl) trifluorophosphate as base oil additive in the lubrication of TiN PVD coating. *Tribol. Int.* **2011**, *44*, 645–650. [[CrossRef](#)]
32. Blanco, D.; Battez, A.H.; Viesca, J.L.; González, R.; Fernández-González, A. Lubrication of CrN coating with ethyl-dimethyl-2-methoxyethylammonium tris(pentafluoroethyl)trifluorophosphate ionic liquid as additive to PAO 6. *Tribol. Lett.* **2011**, *41*, 295–302. [[CrossRef](#)]
33. Viesca, J.L.; García, A.; Hernández Battez, A.; González, R.; Monge, R.; Fernández-González, A.; Hadfield, M. FAP- anion ionic liquids used in the lubrication of a steel-steel contact. *Tribol. Lett.* **2013**, *52*, 431–437. [[CrossRef](#)]
34. Minami, I.; Kita, M.; Kubo, T.; Nanao, H.; Mori, S. The tribological properties of ionic liquids composed of trifluorotris(pentafluoroethyl) phosphate as a hydrophobic anion. *Tribol. Lett.* **2008**, *30*, 215–223. [[CrossRef](#)]
35. Otero, I.; López, E.R.; Reichelt, M.; Fernández, J. Friction and anti-wear properties of two tris(pentafluoroethyl) trifluorophosphate ionic liquids as neat lubricants. *Tribol. Int.* **2014**, *70*, 104–111. [[CrossRef](#)]
36. Viesca, J.L.; Hernández Battez, A.; González, R.; Reddyhoff, T.; Torres Pérez, A.; Spikes, H.A. Assessing boundary film formation of lubricant additived with 1-hexyl-3-methylimidazolium tetrafluoroborate using ECR as qualitative indicator. *Wear* **2010**, *269*, 112–117. [[CrossRef](#)]
37. Hernández Battez, A.; González, R.; Viesca, J.L.; Fernández-González, A.; Hadfield, M. Lubrication of PVD coatings with ethyl-dimethyl-2-methoxyethylammonium tris(pentafluoroethyl)trifluorophosphate. *Tribol. Int.* **2013**, *58*, 71–78. [[CrossRef](#)]
38. Somers, A.E.; Biddulph, S.M.; Howlett, P.C.; Sun, J.; MacFarlane, D.R.; Forsyth, M. A comparison of phosphorus and fluorine containing IL lubricants for steel on aluminium. *Phys. Chem. Chem. Phys.* **2012**, *14*, 8224. [[CrossRef](#)]
39. Viesca, J.L.; Anand, M.; Blanco, D.; Fernández-González, A.; García, A.; Hadfield, M. Tribological behaviour of PVD coatings lubricated with a FAP- anion-based ionic liquid used as an additive. *Lubricants* **2016**, *4*, 8. [[CrossRef](#)]

40. Kheireddin, B.A.; Lu, W.; Chen, I.C.; Akbulut, M. Inorganic nanoparticle-based ionic liquid lubricants. *Wear* **2013**, *303*, 185–190. [[CrossRef](#)]
41. Pisarova, L.; Gabler, C.; Dörr, N.; Pittenauer, E.; Allmaier, G. Thermo-oxidative stability and corrosion properties of ammonium based ionic liquids. *Tribol. Int.* **2012**, *46*, 73–83. [[CrossRef](#)]
42. Cai, M.; Liang, Y.; Yao, M.; Xia, Y.; Zhou, F.; Liu, W. Imidazolium ionic liquids as antiwear and antioxidant additive in poly(ethylene glycol) for steel/steel contacts. *ACS Appl. Mater. Interfaces* **2010**, *2*, 870–876. [[CrossRef](#)] [[PubMed](#)]
43. Gabler, C.; Dörr, N.; Allmaier, G. Influence of cationic moieties on the tribolayer constitution shown for bis(trifluoromethylsulfonyl) imide based ionic liquids studied by X-ray photoelectron spectroscopy. *Tribol. Int.* **2014**, *80*, 90–97. [[CrossRef](#)]
44. Monge, R.; González, R.; Hernández Battez, A.; Fernández-González, A.; Viesca, J.L.; García, A.; Hadfield, M. Ionic liquids as an additive in fully formulated wind turbine gearbox oils. *Wear* **2015**, *328–329*, 50–63. [[CrossRef](#)]
45. Somers, A.E.; Howlett, P.C.; Sun, J.; MacFarlane, D.R.; Forsyth, M. Transition in wear performance for ionic liquid lubricants under increasing load. *Tribol. Lett.* **2010**, *40*, 279–284. [[CrossRef](#)]
46. Murakami, T.; Kaneda, K.; Nakano, M.; Korenaga, A.; Mano, H.; Sasaki, S. Tribological properties of Fe<sub>7</sub>Mo<sub>6</sub>-based alloy under two ionic liquid lubrications. *Tribol. Int.* **2008**, *41*, 1083–1089. [[CrossRef](#)]
47. Bandeira, P.; Monteiro, J.; Baptista, A.M.; Magalhães, F.D. Tribological performance of PTFE-based coating modified with microencapsulated [HMIM][NTf<sub>2</sub>] ionic liquid. *Tribol. Lett.* **2015**, *59*, 13. [[CrossRef](#)]
48. Somers, A.E.; Khemchandani, B.; Howlett, P.C.; Sun, J.; Macfarlane, D.R.; Forsyth, M. Ionic liquids as antiwear additives in base oils: Influence of structure on miscibility and antiwear performance for steel on aluminum. *ACS Appl. Mater. Interfaces* **2013**, *5*, 11544–11553. [[CrossRef](#)]
49. Minami, I.; Inada, T.; Sasaki, R.; Nanao, H. Tribo-chemistry of phosphonium-derived ionic liquids. *Tribol. Lett.* **2010**, *40*, 225–235. [[CrossRef](#)]
50. Amiril, S.A.S.; Rahim, E.A.; Syahrullail, S. A review on ionic liquids as sustainable lubricants in manufacturing and engineering: Recent research, performance, and applications. *J. Clean. Prod.* **2017**, *168*, 1571–1589. [[CrossRef](#)]
51. Qu, J.; Bansal, D.G.; Yu, B.; Howe, J.Y.; Luo, H.; Dai, S.; Li, H.; Blau, P.J.; Bunting, B.G.; Mordukhovich, G.; et al. Antiwear performance and mechanism of an oil-miscible ionic liquid as a lubricant additive. *ACS Appl. Mater. Interfaces* **2012**, *4*, 997–1002. [[CrossRef](#)]
52. Barnhill, W.C.; Qu, J.; Luo, H.; Meyer, H.M.; Ma, C.; Chi, M.; Papke, B.L. Phosphonium-organophosphate ionic liquids as lubricant additives: Effects of cation structure on physicochemical and tribological characteristics. *ACS Appl. Mater. Interfaces* **2014**, *6*, 22585–22593. [[CrossRef](#)] [[PubMed](#)]
53. Anand, M.; Hadfield, M.; Viesca, J.L.; Thomas, B.; Hernández Battez, A.; Austen, S. Ionic liquids as tribological performance improving additive for in-service and used fully-formulated diesel engine lubricants. *Wear* **2015**, *334–335*, 67–74. [[CrossRef](#)]
54. Otero, I.; López, E.R.; Reichelt, M.; Villanueva, M.; Salgado, J.; Fernández, J. Ionic liquids based on phosphonium cations as neat lubricants or lubricant additives for a steel/steel contact. *ACS Appl. Mater. Interf.* **2014**, *6*, 13115–13128. [[CrossRef](#)] [[PubMed](#)]
55. Qu, J.; Luo, H.; Chi, M.; Ma, C.; Blau, P.J.; Dai, S.; Viola, M.B. Comparison of an oil-miscible ionic liquid and ZDDP as a lubricant anti-wear additive. *Tribol. Int.* **2014**, *71*, 88–97. [[CrossRef](#)]
56. Totolin, V.; Minami, I.; Gabler, C.; Brenner, J.; Dörr, N. Lubrication mechanism of phosphonium phosphate ionic liquid additive in alkylborane-imidazole complexes. *Tribol. Lett.* **2014**, *53*, 421–432. [[CrossRef](#)]
57. Zhang, S.; Hu, L.; Qiao, D.; Feng, D.; Wang, H. Vacuum tribological performance of phosphonium-based ionic liquids as lubricants and lubricant additives of multialkylated cyclopentanes. *Tribol. Int.* **2013**, *66*, 289–295. [[CrossRef](#)]
58. Barnhill, W.C.; Luo, H.; Meyer, H.M.; Ma, C.; Chi, M.; Papke, B.L. Tertiary and quaternary ammonium-phosphate ionic liquids as lubricant additives. *Tribol. Lett.* **2016**, *63*, 22. [[CrossRef](#)]
59. Qu, J.; Barnhill, W.C.; Luo, H.; Meyer, H.M.; Leonard, D.N.; Landauer, A.K.; Kheireddin, B.; Gao, H.; Papke, B.L.; Dai, S. Synergistic effects between phosphonium-alkylphosphate ionic liquids and zinc dialkyldithiophosphate (ZDDP) as lubricant additives. *Adv. Mater.* **2015**, *27*, 4767–4774. [[CrossRef](#)]
60. González, R.; Bartolomé, M.; Blanco, D.; Viesca, J.L.; Fernández-González, A.; Battez, A.H. Effectiveness of phosphonium cation-based ionic liquids as lubricant additive. *Tribol. Int.* **2016**, *98*, 82–93. [[CrossRef](#)]
61. Lu, Q.; Wang, H.; Ye, C.; Liu, W.; Xue, Q. Room temperature ionic liquid 1-ethyl-3-hexylimidazoliumbis(trifluoromethylsulfonyl)-imide as lubricant for steel/steel contact. *Tribol. Int.* **2004**, *37*, 547–552. [[CrossRef](#)]
62. Hernández Battez, A.; Bartolomé, M.; Blanco, D.; Viesca, J.L.; Fernández-González, A.; González, R. Phosphonium cation-based ionic liquids as neat lubricants: Physicochemical and tribological performance. *Tribol. Int.* **2016**, *95*, 118–131. [[CrossRef](#)]
63. Otero, I.; López, E.R.; Reichelt, M.; Fernández, J. Tribo-chemical reactions of anion in pyrrolidinium salts for steel-steel contact. *Tribol. Int.* **2014**, *77*, 160–170. [[CrossRef](#)]
64. Hernández Battez, A.; Blanco, D.; Fernández-González, A.; Mallada, M.T.; González, R.; Viesca, J.L. Friction, wear and tribofilm formation with a [NTf<sub>2</sub>] anion-based ionic liquid as neat lubricant. *Tribol. Int.* **2016**, *103*, 73–86. [[CrossRef](#)]
65. Itoga, M.; Aoki, S.; Suzuki, A.; Yoshida, Y.; Fujinami, Y.; Masuko, M. Toward resolving anxiety about the accelerated corrosive wear of steel lubricated with the fluorine-containing ionic liquids at elevated temperature. *Tribol. Int.* **2016**, *93*, 640–650. [[CrossRef](#)]
66. Qu, J.; Blau, P.J.; Dai, S.; Luo, H.; Meyer, H.M., III; Truhan, J.J. Tribological characteristics of aluminum alloys sliding against steel lubricated by ammonium and imidazolium ionic liquids. *Wear* **2009**, *267*, 1226–1231. [[CrossRef](#)]

67. Zhang, H.; Xia, Y.; Yao, M.; Jia, Z.; Liu, Z. The influences of methyl group at C2 position in imidazole ring on tribological properties. *Tribol. Lett.* **2009**, *36*, 105–111. [[CrossRef](#)]
68. Jiménez, A.E.; Bermúdez, M.D.; Carrión, F.J.; Martínez-Nicolás, G. Room temperature ionic liquids as lubricant additives in steel-aluminium contacts: Influence of sliding velocity, normal load and temperature. *Wear* **2006**, *261*, 347–359. [[CrossRef](#)]
69. Mo, Y.; Zhao, W.; Zhu, M.; Bai, M. Nano/microtribological properties of ultrathin functionalized imidazolium wear-resistant ionic liquid films on single crystal silicon. *Tribol. Lett.* **2008**, *32*, 143–151. [[CrossRef](#)]
70. Iglesias, P.; Bermúdez, M.D.; Carrión, F.J.; Martínez-Nicolás, G. Friction and wear of aluminium–steel contacts lubricated with ordered fluids-neutral and ionic liquid crystals as oil additives. *Wear* **2004**, *256*, 386–392. [[CrossRef](#)]
71. Han, Y.; Qiao, D.; Zhang, L.; Feng, D. Study of tribological performance and mechanism of phosphonate ionic liquids for steel / aluminum contact. *Tribol. Int.* **2015**, *84*, 71–80. [[CrossRef](#)]
72. Zeng, Z.; Chen, Y.; Wang, D.; Zhang, J. Tribological behaviors of amorphous Cr coatings electrodeposited from Cr (III) baths under ionic liquid lubrication. *Electrochem. Solid State Lett.* **2007**, *10*, D85–D87. [[CrossRef](#)]
73. Espinosa, T.; Sanes, J.; Jiménez, A.E.; Bermúdez, M.D. Protic ammonium carboxylate ionic liquid lubricants of OFHC copper. *Wear* **2013**, *303*, 495–509. [[CrossRef](#)]
74. Xia, Y.; Sasaki, S.; Murakami, T.; Nakano, M.; Shi, L.; Wang, H. Ionic liquid lubrication of electrodeposited nickel-Si<sub>3</sub>N<sub>4</sub> composite coatings. *Wear* **2007**, *262*, 765–771. [[CrossRef](#)]
75. Kondo, Y.; Koyama, T.; Tsuboi, R.; Nakano, M.; Miyake, K.; Sasaki, S. Tribological performance of halogen-free ionic liquids as lubricants of hard coatings and ceramics. *Tribol. Lett.* **2013**, *51*, 243–249. [[CrossRef](#)]
76. Jiménez, A.E.; Bermúdez, M.D. Ionic liquids as lubricants of titanium–steel contact. *Tribol. Lett.* **2009**, *33*, 111–126. [[CrossRef](#)]
77. Liu, W.; Ye, C.; Chen, Y.; Ou, Z.; Sun, D.C. Tribological behavior of sialon ceramics sliding against steel lubricated by fluorine-containing oils. *Tribol. Int.* **2002**, *35*, 503–509. [[CrossRef](#)]
78. Smiglak, M.; Metlen, A.; Rogers, R.D. The second evolution of ionic liquids: From solvents and separations to advanced materials—energetic examples from the ionic liquid cookbook. *Acc. Chem. Res.* **2007**, *40*, 1182–1192. [[CrossRef](#)]
79. Costa, S.P.F.; Azevedo, A.M.O.; Pinto, P.C.A.G.; Saraiva, M.L.M.F.S. Environmental impact of ionic liquids: Recent advances in (eco)toxicology and (bio)degradability. *ChemSusChem* **2017**, *10*, 2321–2347. [[CrossRef](#)]
80. Reeves, C.J.; Garvey, S.; Menezes, P.L.; Dietz, M.; Jen, T.C.; Lovell, M.R. Tribological performance of environmentally friendly ionic liquid lubricants. *Am. Soc. Mech. Eng. Tribol. Div. TRIB.* **2012**, 355–357. [[CrossRef](#)]
81. Wang, A.; Chen, L.; Jiang, D.; Zeng, H.; Yan, Z. Vegetable oil-based ionic liquid microemulsion biolubricants: Effect of integrated surfactants. *Ind. Crops Prod.* **2014**, *62*, 515–521. [[CrossRef](#)]
82. Syahir, A.Z.; Zulkifli, N.W.M.; Masjuki, H.H.; Kalam, M.A.; Alabdulkarem, A.; Gulzar, M.; Khuong, L.S.; Harith, M.H. A review on bio-based lubricants and their applications. *J. Clean. Prod.* **2017**, *168*, 9971016. [[CrossRef](#)]
83. Adawiyah, N.; Hawatulaila, S.; Aini, A.; Vijaya, A.; Ibrahim, M.; Moniruzzaman, M. Synthesis, characterization, ecotoxicity and biodegradability evaluations of novel bio-compatible surface active lauroyl sarcosinate ionic liquids. *Chemosphere* **2019**, *229*, 349–357. [[CrossRef](#)]
84. Parmentier, D.; Metz, S.J.; Kroon, M.C. Tetraalkylammonium oleate and linoleate based ionic liquids: Promising extractants for metal salts. *Green Chem.* **2013**, *15*, 205–209. [[CrossRef](#)]
85. Rocha, M.A.A.; Bruinhorst, A.V.D.; Schröer, W.; Rathke, B.; Kroon, M.C. Physico-chemical properties of fatty acid based ionic liquids. *J. Chem. Thermodyn.* **2016**, *100*, 156–164. [[CrossRef](#)]
86. Gusain, R.; Dhingra, S.; Khatri, O.P. Fatty-acid-constituted halogen-free ionic liquids as renewable, environmentally friendly, and high-performance lubricant additives. *Ind. Eng. Chem. Res.* **2016**, *55*, 856–865. [[CrossRef](#)]
87. Gusain, R.; Khatri, O.P. Fatty acid ionic liquids as environmentally friendly lubricants for low friction and wear. *RSC Adv.* **2016**, *6*, 3462–3469. [[CrossRef](#)]
88. Mezzetta, A.; Guazzelli, L.; Seggiani, M.; Pomelli, C.S.; Puccini, M.; Chiappe, C. A general environmentally friendly access to long chain fatty acid ionic liquids (LCFA-ILs). *Green Chem.* **2017**, *19*, 3103–3111. [[CrossRef](#)]
89. Fan, M.; Ma, L.; Zhang, C.; Wang, Z.; Ruan, J.; Han, M.; Ren, Y.; Zhang, C.; Yang, D.; Zhou, F.; et al. Biobased green lubricants: Physicochemical, tribological and toxicological properties of fatty acid ionic liquids. *Tribol. Trans.* **2017**, *61*, 195–206. [[CrossRef](#)]
90. Khatri, P.K.; Aathira, M.S.; Thakre, G.D.; Jain, S.L. Synthesis and tribological behavior of fatty acid constituted tetramethylguanidinium (TMG) ionic liquids for a steel/steel contact. *Mater. Sci. Eng. C* **2018**, *91*, 208–217. [[CrossRef](#)]
91. Zheng, G.; Ding, T.; Huang, Y.; Zheng, L.; Ren, T. Fatty acid based phosphite ionic liquids as multifunctional lubricant additives in mineral oil and refined vegetable oil. *Tribol. Int.* **2018**, *123*, 316–324. [[CrossRef](#)]
92. Blanco, D.; Rivera, N.; Oulego, P.; Díaz, M.; González, R.; Battez, A.H. Novel fatty acid anion-based ionic liquids: Contact angle, surface tension, polarity fraction and spreading parameter. *J. Mol. Liq.* **2019**, *288*, 110995. [[CrossRef](#)]
93. Rivera, N.; Blanco, D.; Viesca, J.L.; Fernández-González, A.; González, R.; Battez, A.H. Tribological performance of three fatty acid anion-based ionic liquids (FAILs) used as lubricant additive. *J. Mol. Liq.* **2019**, *296*, 111881. [[CrossRef](#)]
94. Khan, A.; Gusain, R.; Sahai, M.; Khatri, O.P. Fatty acids-derived protic ionic liquids as lubricant additive to synthetic lube base oil for enhancement of tribological properties. *J. Mol. Liq.* **2019**, *293*, 111444. [[CrossRef](#)]
95. Rivera, N.; García, A.; Fernández-González, A.; Blanco, D.; González, R.; Battez, A.H. Tribological behavior of three fatty acid ionic liquids in the lubrication of different material pairs. *J. Mol. Liq.* **2019**, *296*, 111858. [[CrossRef](#)]

96. Ali, K.; Moshikur, R.; Wakabayashi, R.; Tahara, Y. Synthesis and characterization of choline—Fatty-acid-based ionic liquids: A new biocompatible surfactant. *J. Colloid. Interface Sci.* **2019**, *551*, 72–80. [[CrossRef](#)]
97. Oulego, P.; Faes, J.; González, R.; Viesca, J.L.; Blanco, D.; Battez, A.H. Relationships between the physical properties and biodegradability and bacteria toxicity of fatty acid-based ionic liquids. *J. Mol. Liq.* **2019**, *292*, 111451. [[CrossRef](#)]
98. Gundolf, T.; Weyhing-Zerrer, N.; Sommer, J.; Kalb, R.; Schoder, D.; Rossmannith, P.; Mester, P. Biological impact of ionic liquids based on sustainable fatty acid anions examined with a tripartite test system. *ACS Sustain. Chem. Eng.* **2019**, *7*, 15865–15873. [[CrossRef](#)]
99. Gusain, R.; Khan, A.; Khatri, O.P. Fatty acid-derived ionic liquids as renewable lubricant additives: Effect of chain length and unsaturation. *J. Mol. Liq.* **2020**, *301*, 112322. [[CrossRef](#)]
100. Sernaglia, M.; Blanco, D.; Hernández Battez, A.; Viesca, J.L.; González, R.; Bartolomé, M. Two fatty acid anion-based ionic liquids—Part I: Physicochemical properties and tribological behavior as neat lubricants. *J. Mol. Liq.* **2020**, *305*, 112827. [[CrossRef](#)]
101. Reeves, C.J.; Menezes, P.L.; Jen, T.C.; Lovell, M.R. The influence of fatty acids on tribological and thermal properties of natural oils as sustainable biolubricants. *Tribol. Int.* **2015**, *90*, 123–134. [[CrossRef](#)]
102. Saurin, N.; Minami, I.; Sanes, J.; Bermúdez, M.D. Study of the effect of the effect of tribo-materials and surface finish on the lubricant performance of new halogen-free ionic liquids. *Appl. Surf. Sci.* **2016**, *366*, 464–474. [[CrossRef](#)]
103. Gusain, R.; Panda, S.; Bakshi, P.S.; Gardas, R.L.; Khatri, O.P. Thermophysical properties of trioctylalkylammonium bis(salicylate)borate ionic liquids: Effect of alkyl chain length. *J. Mol. Liq.* **2018**, *269*, 540–546. [[CrossRef](#)]
104. Battez, A.H.; Rivera, N.; Blanco, D.; Oulego, P.; Viesca, J.L.; González, R. Physicochemical, traction and tribofilm formation properties of three octanoate-, laurate- and palmitate-anion based ionic liquids. *J. Mol. Liq.* **2019**, *284*, 639–646. [[CrossRef](#)]
105. Sernaglia, M.; Blanco, D.; Hernández Battez, A.; González, R.; Fernández-González, A.; Bartolomé, M. Two fatty acid anion-based ionic liquids—Part II: Effectiveness as an additive to a polyol ester. *J. Mol. Liq.* **2020**, *310*, 113158. [[CrossRef](#)]
106. Liu, Y.; Ma, C.; Men, S.; Jin, Y. An investigation of trioctylmethylammonium ionic liquids by X-ray photoelectron spectroscopy: The cation-anion interaction. *J. Electron Spectrosc. Relat. Phenom.* **2018**, *223*, 79–83. [[CrossRef](#)]
107. Jiang, Y.; Zhang, X.; Al Mehedi, A.; Yang, M.; Wang, J.P. A method to evaluate  $\alpha''$ -Fe<sub>16</sub>N<sub>2</sub> volume ratio in FeN bulk material by XPS. *Mater. Res. Express* **2015**, *2*, 116103. [[CrossRef](#)]
108. Wang, C.; Tao, Q.; Li, Y.; Ma, S.; Dong, S.; Cui, T.; Zhu, P. Excellent mechanical properties of metastable c-WN fabricated at high pressure and high temperature. *Int. J. Refract. Met. Hard Mater.* **2017**, *66*, 63–67. [[CrossRef](#)]
109. Wanner, S.; Hilaire, L.; Wehrer, P.; Hindermann, J.P.; Maire, G. Obtaining tungsten carbides from tungsten bipyridine complexes via low temperature thermal treatment. *Appl. Catal. A Gen.* **2000**, *203*, 55–70. [[CrossRef](#)]
110. Lisowski, W.; van den Berg, A.H.J.; Kip, G.A.M.; Hanekamp, L.J. Characterization of tungsten tips for STM by SEM/AES/XPS. *Fresenius J. Anal Chem.* **1991**, *341*, 196–199. [[CrossRef](#)]